

# Microstructural Observations in a Cast Al-Si-Cu/TiC Composite

A.E. Karantzalis, A. Lekatou, E. Georgatis, V. Poulas, and H. Mavros

(Submitted January 7, 2009; in revised form May 17, 2009)

**A 3-5 vol.% TiC particulate Al-Si-Cu composite was prepared by diluting Al/20 vol.% TiC composite in an Al-7Si-4Cu alloy matrix. TiC particle distribution consists of isolated and clustered particles which are both located at the primary- $\alpha$  grain boundaries and at the areas of the last solidified liquid. Particle pushing by the solidification front is responsible for the final particle location. The solidified microstructure consists of primary and intermetallic phases formed by a sequence of possible eutectic reactions. No evidence of TiC particle degradation was observed.**

**Keywords** Al-alloy cast structures, Aluminum matrix composites, Particle-melt interactions, Particle-solidifying front interactions, TiC particulates, Wetting

## 1. Introduction

During the last four decades, Particulate Reinforced Aluminum Matrix Composites (PRAMCs) have gained great research attention as attractive materials for potential industrial applications. This interest stems from property improvements, regarding strength and stiffness, density, high temperature properties, abrasion, and wear resistance, and damping capacities (Ref 1).

Quite a few different manufacturing and processing routes have been explored and proposed, based either on solid or liquid matrix state. The stir casting process is one of the most important ones, mainly due to cost and ease-to-handle considerations. An extensive research effort has been conducted, to investigate and understand the various phenomena governing the particle-matrix interactions during and after the solidification process. A thorough, in-depth review for these phenomena can be found in the study of Rohatgi et al. (Ref 2). It is considered necessary, however, to address the main aspects concerning the final microstructure of a stir-cast metal matrix composite (Ref 1-6).

Two fundamental phenomena are responsible for the particle distribution and the final microstructure, and, consequently, the composite properties and performance. These are: the particle-liquid metal interactions and the particle-solidification front interactions.

Regarding the particle-molten metal interactions, the particle-melt compatibility influences the initial particle distribution within the liquid melt. The particle-melt compatibility is assessed by means of wettability, i.e., the tendency of the liquid

melt to spread over the surface of a ceramic substrate forming a low ( $<90^\circ$ ) contact angle during the well-known sessile drop experiment (Ref 3, 5, 6). The involved surfaces may be poisoned by oxide phases or absorbed gases. Especially in the case of Al alloys and TiC, the presence of oxides and/or absorbed gases can significantly change their wetting characteristics and their absence can make the wetting of TiC by Al very spontaneous (Ref 7, 8).

Regarding the particle-solidification front interactions, these influence the final particle distribution and location. The particles can be pushed by the solidification front, engulfed by the solidification front or act as solid phase nucleation sites. Many theories have been developed concerning the solidifying front-reinforcing particles interactions, which are based on thermodynamic and kinetic considerations. Zubko et al. (Ref 9) proposed the thermal conductivity criterion, according to which, engulfment will occur when the thermal conductivity of the liquid is higher than that of the reinforcing particles. This theory was refined by Surrapa and Rohatgi (Ref 10). An analytical model for the interaction between an insoluble particle and an advancing solid/liquid interface has been presented by Shangguan et al. (Ref 11) where they addressed the concept of the critical velocity of the interface,  $V_{cr}$ , below which the particle will be pushed and above which the particle will be engulfed. They also showed the dependence of  $V_{cr}$  on surface energy changes and particle size. The role of particle size have been extensively addressed in the research effort of Maity et al. (Ref 12) while dealing with transient liquid phase diffusion bonding of an extruded Al6061-SiC composite material.

Many other models have been based on the idea of solidification front critical velocity (Ref 13-18) and Stefanescu and Dhindaw (Ref 19) summarized the parameters affecting the critical velocity for the different cases of solidification conditions (unidirectional-multidirectional) and the different morphologies of the solidification front (planar, cellular, dendritic).

Although a variety of Al-alloys have been investigated as potential matrix systems (Al, Al-Si, Al-Mg, Al-Mg-Si, Al-Cu, etc.), the research studies have mainly concentrated on SiC and Al<sub>2</sub>O<sub>3</sub> particulate reinforcements (Ref 1-6). However, several experimental efforts have focused on the utilization of TiC particles as potential reinforcements of Al alloys. Characteristic

A.E. Karantzalis, A. Lekatou, E. Georgatis, V. Poulas, and H. Mavros, Department of Materials Science and Engineering, University of Ioannina, 45110 Ioannina, Hellas, Greece. Contact e-mail: karantzalis@hotmail.com.

examples which can be considered include the study of Contreras et al. (Ref 20) and Albiter et al. (Ref 21) who produced Al-Mg/TiC and Al-2024/TiC composites, respectively, by melting infiltration techniques, the study of Selcuk and Kennedy (Ref 22) who prepared an Al/TiC master composite of high TiC content (over 50 vol.%) by reaction synthesis of elemental powders, the studies of Shyu and Ho (Ref 23), Premkumar and Chu (Ref 24), Kharti and Koczak (Ref 25), and Sahoo and Koczak (Ref 26) who produced Al/TiC composites through the reaction of carbonaceous gas with Ti dissolved in an Al melt, and the study of Karantzalis et al. (Ref 8) who produced Al/TiC composites by a stir casting process.

TiC particles were chosen as the reinforcing phase because of their properties and metallic character (Ref 27, 28) considered as important factors for sufficient wetting when in contact with aluminum melts without the necessity of interfacial chemical reactivity. Such behavior can lead to great affinity for molten aluminum, reduced tendency for particle agglomeration, good particle distribution in the melt, and development of strong interfaces, free of reaction products.

In this study, the selection of the matrix material was based on its potential applications and solidification features. During the last decades, cast aluminum alloys have extensively been used by the automotive industry for the production of engine components as potential replacements of cast iron (Ref 29). Among these, alloys of the Al-Si-Cu system, such as A319 and 319, have thoroughly been investigated due to their potential use in the automotive (transport) industry (Ref 30). Among the most common applications, are components, such as cylinder blocks, cylinder heads, pistons, and valve lifters.

It is on this basis, where the scope of this study stands viz, to investigate the potential of produce aluminum matrix composites by the facilitation of halide salts, as well as the solidification behavior of a novel matrix-particulate combination. This combination consists of an Al-Si-Cu alloy as the matrix material, and TiC particulates as the reinforcing phase.

## 2. Experimental Procedure

The examined composites were prepared by diluting a quantity of a master composite material in the main matrix alloy. The main matrix alloy was cast Al-7 wt.% Si-4 wt.% Cu, with Fe and Mn being the main impurities (less than 0.8 wt.%, respectively, for each element). The master composite was Al-20 vol.% TiC prepared by a flux-assisted stir casting process. The preparation method involved the addition of the appropriate mixture of  $KBF_4$  and  $K_3AlF_6$  fluxes along with TiC powders ( $-325$  mesh) on the surface of Al melt. The halides salts react with Al and form a layer of slag that dissolves the oxide film from the melt surface. Subsequently, TiC particles and Al melt express their net wetting characteristics allowing the spontaneous insertion of the reinforcement within the molten metal. Yet, the exact details and the scientific background of the technique are a matter of a future publication. The amount of the master composite added was such that to produce a final 3-5 vol.% TiC composite material. The matrix material was heated up to 800 °C in a resistance furnace. The master composite was then added and allowed for few minutes (no more than 5 min) to dissolve and release the TiC particles. The melt was then gently and softly stirred, to ensure restriction

of particle settling due to sedimentation. Finally, the slurry was poured into steel cylindrical molds. Specimens were cut, mounted, and prepared for inspection.

Standard metallographic procedures were applied (grinding by 80, 200, 500, 800, and 1000 SiC grit papers followed by polishing by 6-, 3-, and 1- $\mu$ m diamond suspensions). Metallographic inspection was conducted through the use of a LEICA 4000 optical microscope. Particle content measurements were conducted with the aid of the 'Image J' image analysis software. The technique is based on the calculation of the different area portions of the involved phases, which are colored differently, through the use of the appropriate optical microscope images. XRD analysis was carried out using the Bruker D8 advance x-ray diffractometer with a Cu-K $\alpha$  lamp. SEM inspection was carried out using the JEOL 5600 system equipped with an Oxford Instruments EDS analysis system. The EBSD-SEM image was recorded with the forescatter (FSD) detector system of the EBSD detector (Nordlys II, HKL Ltd.) into a Zeiss Supra35VP FE-SEM.

## 3. Results and Discussion

### 3.1 Particle Distribution

Figure 1 presents an optical micrograph of the composite microstructure at relatively low magnifications. Based on similar micrographs, the TiC volume fraction was calculated by image analysis and found to be within the range of 3-5 vol.%. The microstructure consists of primary- $\alpha$  grains, TiC particles, and several other phases that will be presented in the following sections. The TiC particles appear to have a relatively uniform distribution of both isolated and clustered particles. The vast majority of the TiC particles, in either form, are located at the areas of the last solidified liquid (i.e., the primary  $\alpha$ -grain boundaries). The TiC particles did not act as nucleation sites for primary- $\alpha$  grain. The average size of the primary- $\alpha$  grains is close to 100  $\mu$ m.

Figure 2(a-c) illustrates the microstructure of the alloy under SEM examination. The matrix-ceramic interface does not show

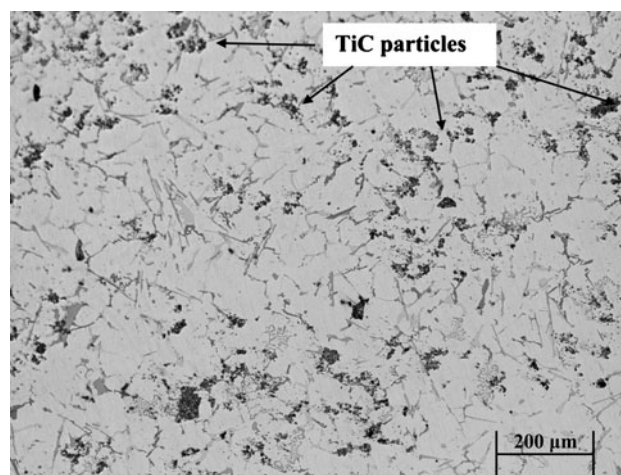
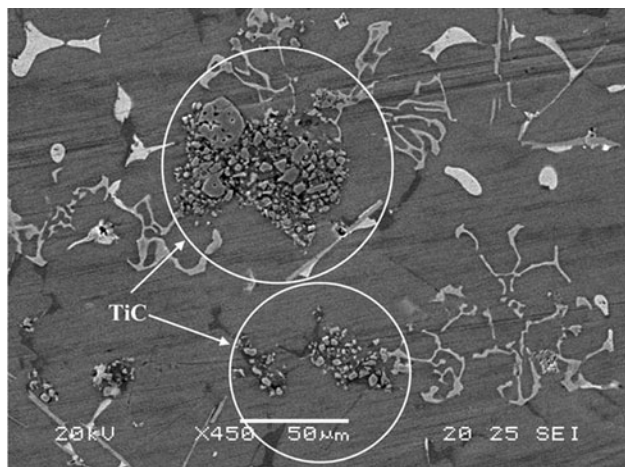


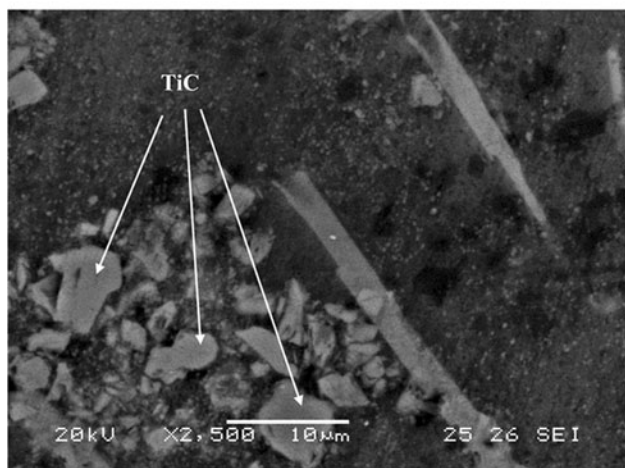
**Fig. 1** Optical micrograph presenting the composite microstructure at a higher magnification. The TiC particles are located at the grain boundaries (i.e., the areas of the lastly solidified liquid). Various different phase constituents are also observed (see Fig. 4, 5)

(at least for this depth of examination) any evidence of particle-degradation reaction to form phases, such as  $\text{Al}_3\text{Ti}$  or  $\text{Al}_4\text{C}_3$ .

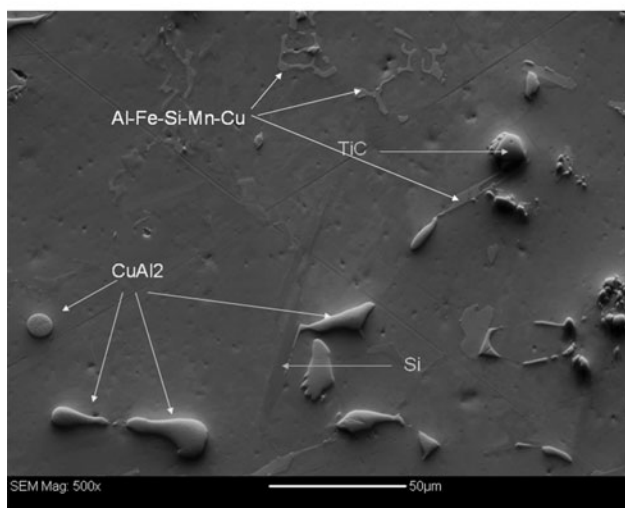
As aforementioned in the introduction section, the key phenomena responsible for the final particle distribution are the



(a)



(b)



(c)

**Fig. 2** The composite microstructure on SEM examination. (a) and (b) SEI image. (c) EBSD image. No signs of TiC-matrix interactions are discerned

melt-particle interactions and the solidifying front-particle interactions.

**3.1.1 Melt-Particle Interactions.** The uniform dispersion of the ceramic particles in the molten matrix is a crucial factor for the resulting microstructure and is directly linked with the wetting characteristics of the involved phases. Good wetting is primarily responsible for the introduction of the ceramic phase into the molten alloy. TiC is a compound of strong metallic nature owing to the presence of Ti. Such a metallic character is reported to improve the wetting behavior of TiC when in contact with metallic melts (Ref 27, 28). The Al-TiC wetting behavior is somehow more complicated. In general, the system is characterized by good wettability, low contact angles, and good interfacial bonding (Ref 31). However, such behavior is achieved only when the surface oxide layer covering the Al melt is removed or dissociated. This removal or dissociation occurs only at high temperatures ( $>900\text{ }^\circ\text{C}$ ) (Ref 31). At such high temperatures, the system becomes intensively reactive; the dissociation of TiC and the formation of  $\text{Al}_4\text{C}_3$  and/or  $\text{Al}_3\text{Ti}$  compounds take place at or close to the interfacial area (Ref 27, 32). In general, such reactivity improves wettability (Ref 27, 28); however, the formation of new phases can alter dramatically the nature and the response of the reinforcement-matrix interface. Such formation has not been observed in this study. This is probably attributed to the short processing time.

The use of fluxes in the production of the master composite ensures minimization of the oxide phases (Ref 7, 8) and consequent improvement of the wetting behavior. This beneficial action is attributed to the ability of the formed slag to dissolve the oxide phases present on the surface of the melt. Such a good wetting may lead to a good particle distribution within the molten alloy. The clusters observed could be either inherited by the precursor master composite or be a result of the solidifying front-particle interactions, as discussed in section 3.1.2.

During conventional manufacturing of cast metal matrix composites, extensive mechanical stirring is used to provide the necessary shear forces for both reinforcing phase insertion and precursor material clusters dissociation. In this study, such a mechanical stirring was not adopted because the main target of the effort was to evaluate the ability of the salts to introduce the ceramic phase within the melt in the absence of any other supportive mechanism.

**3.1.2 Solidifying Front-Particle Interactions.** Besides facing the melt during solidification, the TiC particles are also facing the solidifying front. This interaction also plays a crucial role in particle distribution and final microstructure.

Figure 1 shows a preferential location of TiC particles at the primary  $\alpha$ -grain boundaries associated with eutectic and intermetallic phases. (The nature of the phases is discussed in section 3.2.) Therefore, it is postulated that the first phase to solidify is primary- $\alpha$ . The primary- $\alpha$  grains push the TiC particles to the end to solidify liquid areas. In this case, the so-called thermal conductivity model, proposed by Zubko et al. (Ref 9) and refined by Surappa and Rohatgi (Ref 10), appears sufficiently applicable. During cooling, the thermal conductivity difference between TiC [ $20.5\text{ W/m K}$  (Ref 33)] and Al melt [ $90\text{ W/m K}$  at  $660\text{ }^\circ\text{C}$  (Ref 34)] causes the liquid at the particle periphery to be at higher temperature than the rest of the melt. Hence, the solid phase prefers to start its nucleation away from the particle surface, at particle-free melt areas. Consequently, the TiC particles are blocked within the last solidified liquid, where eutectic and other intermetallic phases are present. This

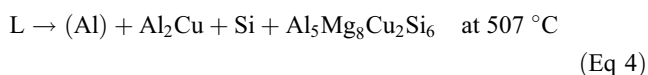
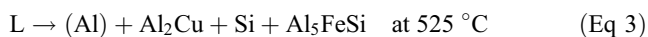
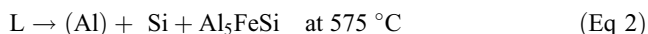
TiC particle rejection at the grain boundaries can also be a reason for cluster formation.

### 3.2 Microstructural Constituents

Figure 3 presents the XRD spectrum of the as-cast composite.  $\alpha$ -Al, Si, TiC, and  $\text{CuAl}_2$  are the dominant phases. Other intermetallic phases have been reported for similar types of alloys, such as  $\text{Al}_5\text{FeSi}$ ,  $\text{Al}_{15}\text{Mn}_3\text{Si}_2$ , etc. (Ref 35). The identification of them by XRD is difficult due to extensive overlapping with the main peaks.

Figure 4(a) shows an optical micrograph of the alloy microstructure. At least three different intermetallic phases have been identified mainly through their morphological features and EDX analysis. Figure 4(b) is an SEM micrograph of the alloy at back scattered mode, where the different phase constituents are clearly discerned. EDX analysis revealed the presence of: Si, TiC,  $\text{CuAl}_2$ ,  $\text{Al}_5\text{FeSi}$ , and another complex intermetallic compound similar to  $\text{Al}_5\text{FeSi}$  but with Mn and Cu present; this compound has the approximate stoichiometry of  $\text{Al}_5\text{FeSiMn}_{0.2}\text{Cu}_{0.2}$ . Si is in the form of acicular or elongated platelets mainly located at the grain boundaries of primary Al. The  $\text{CuAl}_2$  phase is in the form of blocky particles also located at the grain boundaries. The  $\text{Al}_5\text{FeSi}$  has a needle-like structure, whereas the complex intermetallic  $\text{Al}_5\text{FeSiMn}_{0.2}\text{Cu}_{0.2}$  is in the form of the so-called Chinese script. The solidification procedure of an Al-Si hypoeutectic alloy, such as the one used in the present effort, should essentially involve two main stages of solid phase/microconstituent formation: a pre-eutectic stage of primary  $\alpha$ -Al grain formation and a eutectic stage of Al-Si eutectic constituent formation. However, the alloying addition significantly alters the solidification behavior of the alloy, making the sequence of phase formation more complicated.

Figure 5 shows that the presence of intermetallic phases is associated with the presence of TiC. In particular, Fig. 5(a) shows that TiC particles are located at the periphery of  $\text{CuAl}_2$ ,  $\text{Al}_5\text{FeSi}$ , and Si particles. Figure 5(b) reveals strong segregation of TiC particles around Si and  $\text{Al}_5\text{FeSiMn}_{0.2}\text{Cu}_{0.2}$ . Figure 5(c) shows that TiC particles are located at the  $\text{CuAl}_2$  and  $\text{Al}_5\text{FeSiMn}_{0.2}\text{Cu}_{0.2}$  boundaries. Moreover, Fig. 5 shows that the growth of the intermetallic phases is also interrelated to the presence of Si at the primary  $\alpha$ -grain boundaries. In particular, this is illustrated for  $\text{CuAl}_2$ -Si in Fig. 5(a), for  $\text{Al}_5\text{FeSiMn}_{0.2}\text{Cu}_{0.2}$ -Si and  $\text{CuAl}_2$ -Si in Fig. 5(b), and for  $\text{Al}_5\text{FeSiMn}_{0.2}\text{Cu}_{0.2}$ -Si,  $\text{Al}_5\text{FeSi}$ -Si, and  $\text{CuAl}_2$ -Si in Fig. 5(c). The formation of intermetallic particles next to the Si particles may be ascribed to the sequence of solidification reactions in the Al-Si-Cu system proposed by Backerund et al. (Ref 35):



The brackets of  $\text{Al}_5\text{FeSi}$  in Eq 1 mean that its formation at  $590^\circ\text{C}$  was not fully clarified. The last intermetallic was not observed in the present work owing possibly to the small

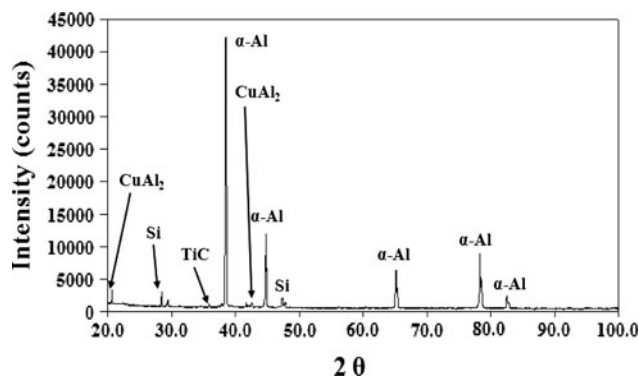
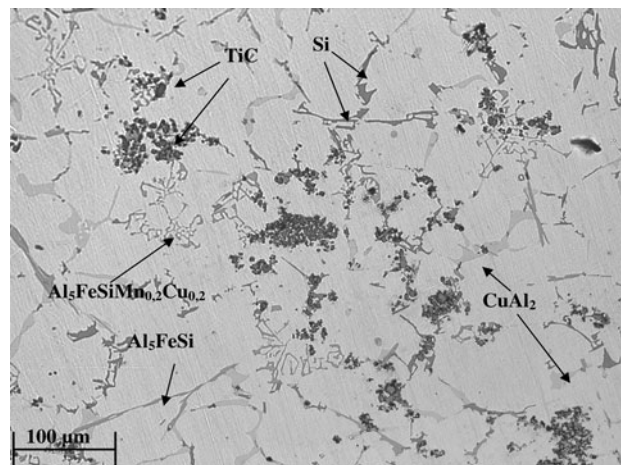
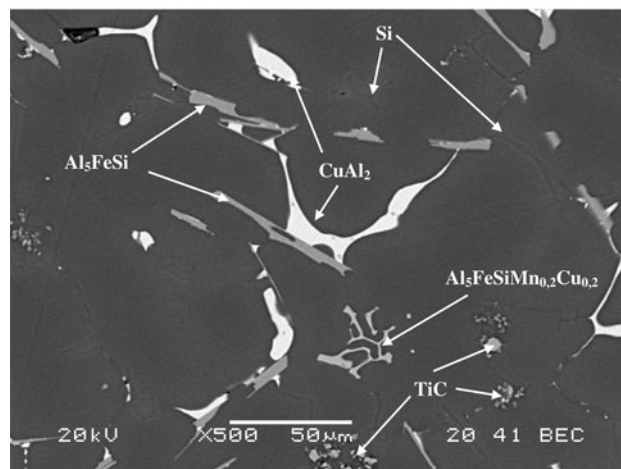


Fig. 3 XRD spectrum of the examined composite



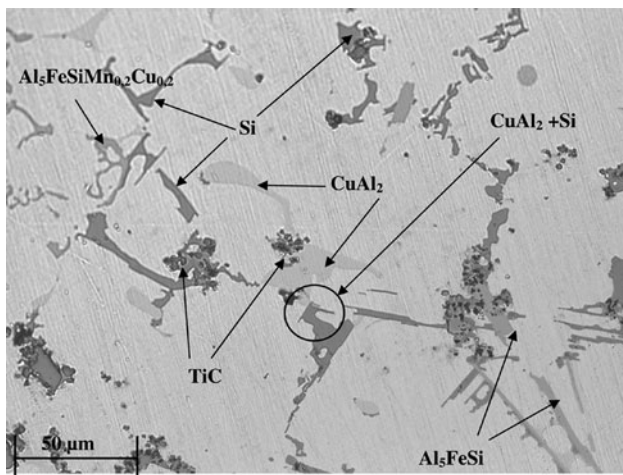
(a)



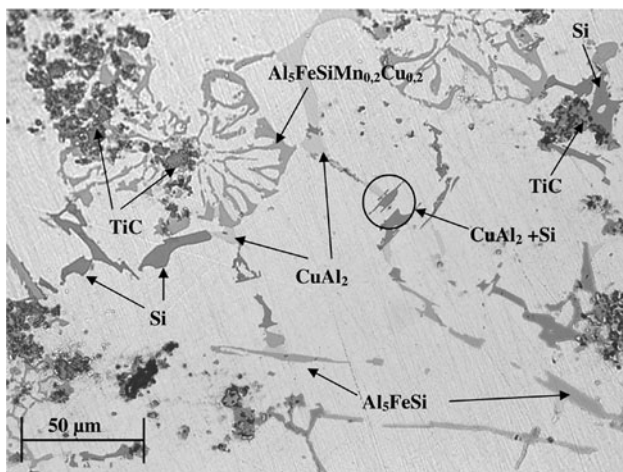
(b)

Fig. 4 (a) Optical micrograph showing the different phases present in the solidified composite.  $\alpha$ -Al, Si,  $\beta$ - $\text{Al}_5\text{FeSi}$ ,  $\text{Al}_5\text{FeSiMn}_{0.2}\text{Cu}_{0.2}$ ,  $\text{CuAl}_2$ , and TiC are observed. (b) SEM back-scattered image showing the different formed phases

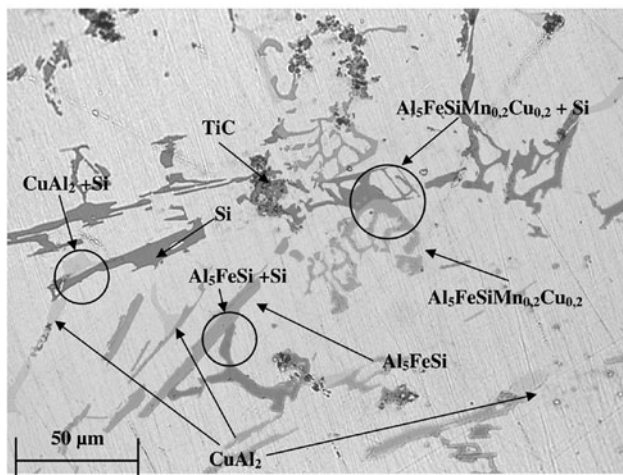
amounts of Mg. Similar observations on the formation of Si and  $\text{CuAl}_2$  have been made by Samuel et al. (Ref 36), although somewhat different temperatures of formation, as well as intermetallic phases are claimed.



(a)



(b)



(c)

**Fig. 5** Optical micrograph of the composite the interrelations of the eutectic phases with TiC and Si particles. (a) TiC-CuAl<sub>2</sub>, TiC-Al<sub>5</sub>FeSi, TiC-Si, CuAl<sub>2</sub>-Si; (b) TiC-Al<sub>5</sub>FeSiMn<sub>0.2</sub>Cu<sub>0.2</sub>, TiC-Si, Al<sub>5</sub>FeSiMn<sub>0.2</sub>Cu<sub>0.2</sub>-Si, CuAl<sub>2</sub>-Si; (c) TiC-CuAl<sub>2</sub>, TiC-Al<sub>5</sub>FeSiMn<sub>0.2</sub>Cu<sub>0.2</sub>, TiC-Si, Al<sub>5</sub>FeSiMn<sub>0.2</sub>Cu<sub>0.2</sub>-Si, Al<sub>5</sub>FeSi-Si, CuAl<sub>2</sub>-Si

Samuel et al. (Ref 36) did not observe the presence of Al<sub>5</sub>FeSi alone but only with the dissolution of other alloying elements in its structure. Mulazimoglu et al. (Ref 37) generally

agreed with the observations of Backerund et al. (Ref 35). None of these studies has mentioned the formation of the complex Al<sub>5</sub>FeSiMn<sub>0.2</sub>Cu<sub>0.2</sub> intermetallic. Its position in the solidification sequence is difficult to be explained, thus needing further experimentation.

The interrelation of the various phases with the TiC particles could be indicative of their role as potential sites for heterogeneous nucleation of various intermetallic phases. This hypothesis is further supported by the presence of TiC particles at the last to solidify areas, where they have been pushed by the solidification front, as aforementioned in section 3.1.2. Furthermore, the presence of eutectic microconstituents in contact with TiC particles enhances the above speculation by suggesting that they have acted as eutectic reaction substrates/catalysts.

In conclusion, the thermal conductivity differences along with the effect of particle size on the solidification front critical velocity satisfyingly explain the TiC particle being pushed to the grain boundaries. On the other hand, the extensive presence of TiC at these lastly solidified liquid areas along with eutectic phases, support a role of heterogeneous nucleation inducer.

This solidification approach does not exclude the occurrence of more complicated eutectic reactions and sequences, and therefore further investigations are required.

## 4. Conclusions

- An Al-20 vol.% TiC master composite was diluted in a matrix of Al-7Si-4Cu resulting in the production of a 3-5 vol.% TiC composite material.
- The good wetting characteristics between TiC particles and the matrix, as those ensured by the use of halide salts during the manufacturing stage, are responsible for the successful particle insertion.
- The preferential placement of TiC particles at the grain boundaries of the primary  $\alpha$ -phase, which present equiaxed morphology, is attributed to particle pushing phenomena by the solidification front. The differences in thermal conductivities and the solidification front critical velocity concept, explain this behavior.
- Various primary and intermetallic phases were developed during solidification. The majority of them are located at the areas of the last solidifying liquid. A possible progress of phase formation is based on sequential eutectic reactions according to which,  $\alpha$ -Al, Si, Al<sub>5</sub>FeSi, Al<sub>5</sub>FeSiMn<sub>0.2</sub>Cu<sub>0.2</sub>, and CuAl<sub>2</sub> are formed.
- The TiC particles have acted as heterogeneous nucleation sites mostly for intermetallic phases.
- TiC has not shown any sign of reaction degradation.

## Acknowledgments

The authors wish to thank Dr. V. Drakopoulos, Principal Scientist of the Institute of Chemical Engineering and High Temperature Process of the Foundation of Research, Greece, for his assistance in the XRD and EBSD—SEM analysis, and Mr. A. Katsoulidis, Post-graduate student of the Chemistry Department of the University of Ioannina, Greece, for his assistance in the SEM examination.

## References

1. D.J. Lloyd, Particle Reinforced Aluminium and Magnesium Matrix Composites, *Int. Mater. Rev.*, 1999, **39**, p 1–23
2. P.K. Rohatgi, R. Asthana, and S. Das, Solidification, Structures and Properties of Cast Metal-Ceramic Particle Composites, *Int. Mater. Rev.*, 1986, **31**, p 115–139
3. A. Mortensen and I. Jin, Solidification Processing of Metal Matrix Composites, *Int. Mater. Rev.*, 1992, **37**, p 101–128
4. P.K. Rohatgi, S. Ray, R. Asthana, and C.S. Narendranath, Interfaces in Cast Metal Matrix Composites, *Mater. Sci. Eng.*, 1993, **A162**, p 163–174
5. R. Asthana and S.N. Tewari, Interfacial and Capillary Phenomena in Solidification Processing of Metal Matrix Composites, *Compos. Manuf.*, 1993, **4**(1), p 3–25
6. J.M. Howe, Bonding, Structure and Properties of Metal/Ceramic Interfaces: Part 1 Chemical Bonding, Chemical Reaction and Interfacial Structure, *Int. Mater. Rev.*, 1993, **38**(5), p 233–256
7. A.R. Kennedy and A.E. Karantzalis, The Incorporation of Ceramic Particles in Molten Aluminium and the Relationship to Contact Angle Data, *Mater. Sci. Eng.*, 1999, **A264**(1–2), p 122–129
8. A.E. Karantzalis, S. Wyatt, and A.R. Kennedy, The Mechanical Properties of Al-TiC Metal Matrix Composites Fabricated by a Flux-Casting Technique, *Mater. Sci. Eng.*, 1997, **A237**(2), p 200–206
9. A.M. Zubko, V.G. Lobanov, and V.V. Nikonova, Reaction of Foreign Particles with a Crystallization Front, *Sov. Phys. Crystallogr.*, 1973, **18**(2), p 239–241
10. M.K. Surrappa and P.K. Rohatgi, Heat Diffusivity Criterion for the Entrapment of Particles by a Moving Solid-Liquid Interface, *J. Mater. Sci.*, 1981, **16**(2), p 562–564
11. D. Sungguan, S. Ahuja, and D.M. Stefanescu, An Analytical Model for the Interaction Between an Insoluble Particle and an Advancing Solid/Liquid Interface, *Metall. Trans. A*, 1992, **23**, p 669–680
12. J. Maity, T.K. Pal, and R. Maiti, Microstructural Characterization of TLPD Bonded 6061-SiCp Composite, *J. Mater. Eng. Perform.*, 2008, **17**(5), p 746–754
13. D.R. Ulmann, B. Chalmers, and K.A. Jackson, Interaction Between Particles and Solid-Liquid Interface, *J. Appl. Phys.*, 1964, **35**(10), p 2986–2993
14. J. Cisse and G.F. Bolling, A Study of the Trapping and Rejection of Insoluble Particles During the Freezing of Water, *J. Cryst. Growth*, 1971, **10**, p 67–76
15. J. Cisse and G.F. Bolling, The Steady State Rejection of Insoluble Particles by Salol Grown from the Melt, *J. Cryst. Growth*, 1971, **11**, p 25–28
16. G.F. Bolling and J. Cisse, A Theory for the Interaction of Particles with Solidifying Front, *J. Cryst. Growth*, 1971, **10**, p 55–66
17. A.A. Chernov, D.E. Temkin, and A.M. Melnikova, Theory of the Capture of Solid Inclusions During the Growth of Crystals from the Melt, *Sov. Phys. Crystallogr.*, 1976, **21**(4), p 369–373
18. D.M. Stefanescu, B.K. Dhindaw, S.A. Kacar, and A. Moitra, Behaviour of Ceramic Particles at the Solid Liquid Metal Interface in Metal Matrix Composites, *Metall. Trans. A*, 1988, **19**, p 2847–2855
19. D.M. Stefanescu and B.K. Dhindaw, Behaviour of Insoluble Particles at the Solid/Liquid Interface, *ASM Metals Handbook*, Vol. 15 Casting, ASM International, 1988, p 315–326, ISBN 0-87170-021-2
20. A. Contreras, C. Angeles-Chávez, O. Flores, and R. Perez, Structural, Morphological and Interfacial Characterization of Al-Mg/TiC Composites, *Mater. Character.*, 2007, **58**, p 685–693
21. A. Albitzer, C.A. Leon, R.A.L. Drew, and E. Bedolla, Microstructure and Heat-treatment Response of Al-2024/TiC Composites, *Mater. Sci. Eng.*, 2000, **A289**, p 109–115
22. C. Selcuk and A.R. Kennedy, Al-TiC Composite Made by the Addition of Master Alloys Pellets Synthesized from Reacted Elemental Powders, *Mater. Lett.*, 2006, **60**, p 3364–3366
23. R.F. Shyu and C.T. Ho, In Situ Reacted Titanium Carbide-reinforced Aluminium Alloys Composite, *J. Mater. Process. Technol.*, 2006, **171**, p 411–416
24. M.K. Premkumar and M.G. Chu, Al-TiC Particulate Composite Produced by a Liquid State In Situ Process, *Mater. Sci. Eng.*, 1995, **A202**, p 172–178
25. S. Khatri and M. Koczak, Formation of TiC in In Situ Processed Composites via Solid-Gas and Liquid-Gas Reactions in Molten Al-Ti, *Mater. Sci. Eng.*, 1993, **A162**, p 153–162
26. P. Sahoo and M. Koczak, Analysis of In Situ Formation of Titanium Carbide in Aluminium Alloys, *Mater. Sci. Eng.*, 1991, **A144**, p 37–44
27. N. Eustathopoulos, M.G. Nicolas, and B. Drevet, Wettability at High Temperatures, Pergamon Materials Series, R.W. Chan, Ed., 1999, p 300, ISBN: 0-08-042146-6
28. J.V. Naidich, The Wettability of Solids by Liquid Metals, *Prog. Surf. Membr. Sci.*, 1981, **14**, p 353–484
29. D. Ovono, I. Guillot, and D. Massinon, The Microstructure and Precipitation Kinetics of a Cast Aluminium Alloy, *Scripta Mater.*, 2006, **55**, p 259–262
30. R. Mahmudi, P. Sepelband, and H.M. Ghasemi, Improved Properties of A319 Aluminium Casting Alloy Modified with Zr, *Mater. Lett.*, 2006, **60**, p 2606–2610
31. S.K. Rhee, Wetting of Ceramics by Liquid Aluminium, *J. Am. Ceram. Soc.*, 1970, **53**(7), p 386–389
32. V.H. Lopez, A. Scoles, and A.R. Kennedy, The Thermal Stability of TiC Particles in an Al 7 wt.% Si Alloy, *Mater. Sci. Eng.*, 2003, **A356**, p 316–325
33. *ASM Metals Handbook, Composites*, Vol. 21, ASM International, 2004, p 132, ISBN 0-87170-703-9
34. *ASM Metals Handbook, Properties and Selection: Non-Ferrous Alloys and Special Purpose Materials*, Vol. 2, ASM International, 1990, p 2924, ISBN 0-87170-378-5
35. L. Backerud, G. Chai, and J. Tamminen, *Solidification Characteristics of Aluminum Alloys*, Foundry Alloys, AFS/Skanaluminium, Des Plaines, IL, 1990, p 127–134
36. F.H. Samuel, A.M. Samuel, and H.W. Doty, Factors Controlling the Type and Morphology of Cu-Containing Phases in 319 Al Alloy, *AFS Trans.*, 1996, **104**, p 893–903
37. M.H. Mulazimoglu, N. Tenekedjiev, B.M. Closset, and J.E. Gruzleski, Studies on the Minor Reactions and Phases in Strontium Treated Aluminium-Silicon Casting Alloys, *Cast Met.*, 1993, **6**, p 16–28